Hindawi Publishing Corporation
Journal of Spectroscopy
Volume 2013, Article ID 471061, 5 pages
http://dx.doi.org/10.1155/2013/471061

Research Article

Vibrational Investigations of Silver-Doped Hydroxyapatite with Antibacterial Properties

Carmen Steluta Ciobanu,[1] Simona Liliana Iconaru,[1] Phillippe Le Coustumer,[2] and Daniela Predoi[1]

[1] *National Institute of Materials Physics, 105 bis Atomistilor, P.O. Box MG 07, Magurele, 077125 Bucharest, Romania*
[2] *Universite Bordeaux, EA 4592 Géoressources & Environnement, EGID, 1 Allée F. Daguin 18, 33607 Pessac Cedex, France*

Correspondence should be addressed to Daniela Predoi; dpredoi@gmail.com

Received 23 June 2012; Accepted 23 July 2012

Academic Editor: Petre Makreski

Silver-doped hydroxyapatite (Ag:HAp) was obtained by coprecipitation method. Transmission electron microscopy (TEM), infrared, and Raman analysis confirmed the development of Ag:HAp with good crystal structure. Transmission electron microscopy analysis showed an uniform ellipsoidal morphology with particles from 5 nm to 15 nm. The main vibrational bands characteristic to HAp were identified. The bands assigned to phosphate vibrational group were highlighted in infrared and Raman spectra. The most intense peak Raman spectrum is the narrow band observed at 960 cm^{-1}. In this article Ag:HAp-NPs were also evaluated for their antimicrobial activities against *gram-positive, gram-negative*, and fungal strains. The specific antimicrobial activity revealed by the qualitative assay demonstrates that our compounds are interacting differently with the microbial targets.

1. Introduction

Nanotechnology is an emerging field which reaches out to develop a bridge between the macroscopic and the atomic or molecular levels of matter. Nowadays the research community looks for answers in the field of nanomaterials for the most pressing problems in medicine, electronics, optics, and environment. The most studied materials are the ones showing similarities and good compatibility with the living tissues due to the large medical applications they qualify for [1–3]. Biomaterials, especially bioceramics belonging to calcium phosphate class, are widely investigated because of their unique properties and high similarities with human osseous tissue. In the last decade a lot of attention was directed towards hydroxyapatite (HAp) from the family of apatites, which is known to be in its natural form a major inorganic constituent of human bones and teeth [4–6]. Having the general formula, Ca_{10} $(PO_4)_6$ $(OH)_2$, HAp has been widely studied for dental and orthopedic applications due to its outstanding properties of osteoconductivity and biocompatibility. In order to be able to meet the high demands that are nowadays required in the field of medical implants, dental implants, or bone tissue reconstruction, biomaterials such as HAp are often improved with other significant elements [7–9]. The HAp structure allows the substitution of Ca^{2+} ions with other metal ions such as Zn^{2+}, Cu^{2+}, and Ag^{+} [10]. As we all know, silver has been widely used since ancient times as an antimicrobial agent. Due to the outbreak of diseases and apparition of drug resistant bacterial strains, in the last years, there have been made extensive studies in order to develop new antibacterial compounds based on the effects of silver against bacterial strains. The antibacterial action of silver nanoparticles is not completely understood and in pure state it has been reported to be toxic towards human organism [11].

The result of substituting Ca^{2+} ions with Ag^{+} ions in the structure of HAp is a new compound which presents high biocompatibility, osteoconductivity, bone regeneration properties, and above all good antibacterial properties [12].

This work presents the results of infrared spectroscopic analysis and Raman investigations of silver-doped hydroxyapatite with x_{Ag} = 0, 0.4, and 0.5. This study represents an

extension of results reported in our previous work [13]. The aim of this study was the evaluation of the antibacterial activity of Ag:HAp nanoparticles when the silver concentration in the samples was increased at 0.4 and 0.5. The structure and morphology of the obtained samples were characterized by transmission electron microscopy (TEM). In vitro qualitative antimicrobial activity of silver-doped hydroxyapatite samples was also investigated.

2. Experimental Section

The synthesis of $(Ca_{10-x}Ag_x)(PO_4)_6(OH)_2$, with $x_{Ag} = 0$, $x_{Ag} = 0.4$ and $x_{Ag} = 0.5$ was carried out as reported in other papers [13]. Transmission electron microscopy (TEM) studies were carried out using an FEI Tecnai 12 equipped with a low-dose digital camera from Gatan. The specimen for TEM imaging was prepared by ultramicrotomy in order to obtain thin section of about 60 nm. The powder is embedded in an epoxy resin (polaron 612) before microtomy. TEM modes used were bright field (BF) and selected area diffraction (SAD). The functional groups present in the prepared nanoparticles and thin films were identified by FTIR using a spectrum BX spectrometer. To obtain the nanoparticles spectra, 1% of the nanopowder was mixed and grounded with 99% KBr. Tablets of 10 mm diameter were prepared by pressing the powder mixture at a load of 5 tons for 2 min. The spectrum was recorded in the range of 500 to 4000 cm^{-1} with 4 cm^{-1} resolution. Micro-Raman spectra on powders were performed in a backscattering geometry at room temperature and in ambient air, under a laser excitation wavelength of 514 nm, using a Jobin Yvon T64000 Raman spectrophotometer under a microscope.

The microbial strains identification was confirmed by aid of VITEK II automatic system. VITEK cards for identification and susceptibility testing were inoculated and incubated according to the manufacturer's recommendations. The results were interpreted using the software version AMS R09.1. Microbial suspensions of 1.5×10^8 CFU/mL corresponding to 0.5 McFarland density obtained from 15–18 h bacterial cultures developed on solid media were used in our experiments. The tested substances were solubilised in DMSO and the starting stock solution was of 5000 μg/mL concentration. The qualitative screening was performed by an adapted disk diffusion method [14–18].

3. Results and Discussions

Figure 1 exhibits the TEM images of pure HAp ($x_{Ag} = 0$) and Ag:HAp ($x_{Ag} = 0.4$, and $x_{Ag} = 0.5$) with low resolution. As shown in Figure 1, pure HAp and Ag:HAp exhibit an ellipsometric morphology, which is consistent with the SEM results [13].

It can be seen from the HRTEM image of Ag:HAp (Figure 2(a)) that the crystalline phase of hydroxyapatite with well-resolved lattice fringes can be observed. The distances between the adjacent lattice fringes (2.72 Å) agree well with the d_{300} spacing of the literature values (2.872 Å) (ICDD-PDF no. 9-432). All 3 samples exhibit a uniform ellipsoidal morphology with particles from 5 nm to 15 nm. The Figure 2(b) shows a selected area electron diffraction (SAED) pattern recorded from an area containing a large number of ellipsometric nanoparticles. The rings in the SAED pattern can be indexed as (002), (210), (211), (310), (222), (213), (004) and (304) reflections of the hexagonal HAp, in agreement with the XRD results. No extra reflections are observed and we can therefore conclude that the product consists of pure HAp ellipsometric nanoparticles.

These results are well consistent with the XRD results [13], revealing that the doping components have little influence on the surface morphology of the samples. The morphology identifications indicated that the nanoparticles with good crystal structure could be made by coprecipitation method at low temperature.

FT-IR spectroscopy was performed in order to investigate the functional groups present in nanohydroxyapatite, $Ca_{10-x}Ag_x(PO_4)_6(OH)_2$, ($x_{Ag} = 0$, 0.4, and 0.5) synthesized at 100°C by coprecipitation method. Figure 3 shows the FT-IR results obtained from Ag:HAp-NPs when the x_{Ag} increases from 0 to 0.5. The absorption peak in the region of 1600–1700 cm^{-1}, ascribed to O–H bending mode, is evidence of the presence of absorbed water in the synthesis products [19–21].

These data clearly revealed the presence of various vibrational modes corresponding to phosphate and hydroxyl groups. For all the samples the presence of strong OH vibration peak could be noticed. The peak observed at 634 cm^{-1} is attributed to the characteristic stretching and vibrational modes of structural OH groups [22, 23]. The band at 1630 cm^{-1} corresponds to the adsorbed H_2O [23].

Bands characteristics of PO_4^{3-} tetrahedral apatite's structure are clearly observed at 473 cm^{-1}, 563 cm^{-1}, 603 cm^{-1}, 960 cm-1, and 1095–1033 cm^{-1} [24, 25]. The peak at 473 cm^{-1} is attributed to $PO_4\nu_2$. The peaks at 563 cm^{-1} and 603 cm^{-1} belong to $PO_4\nu_4$. The peak at 960 cm^{-1} is attributed to $PO_4\nu 1$ and the peaks at 1095–1033 cm^{-1}, are attributed to $PO_4\nu 3$. A CO_3^{2-} band occurred in the spectra at 1452 and 1408 cm^{-1} [26, 27]. The bands at 875 cm^{-1} are attributed to HPO_4^{2-} ions [28–30].

Complementary information can be obtained from Raman spectroscopy. Raman spectra of Ag:HAp from 1200 cm^{-1} to 400 cm^{-1} is shown in Figure 4. The OH^- vibrational bands expected in the region of 630 cm^{-1} are not clearly detected. This behavior is in good accord with the previous studies [31].

We assigned the bands present at 1026 cm^{-1} (ν_3), 1047 cm^{-1} (ν_3), and 1073 cm^{-1} (ν_3) to the asymmetric ν_3 (P–O) stretching. The internal modes of the PO_4^{3-} tetrahedral ν_1 frequency (960 cm^{-1}) corresponds to the symmetric stretching of P–O bonds. The 616 cm^{-1}, 590 cm^{-1}, and 576 cm^{-1} bands arise from ν_4 PO_4 [28]. The vibrational bands at 446 cm^{-1} (ν_2) and 431 cm^{-1} (ν_2) are attributed to the O–P–O bending modes. The band at 1070 cm^{-1} (ν_1) attributed to CO_3^{2-} impurity is by the strong intensity PO_4

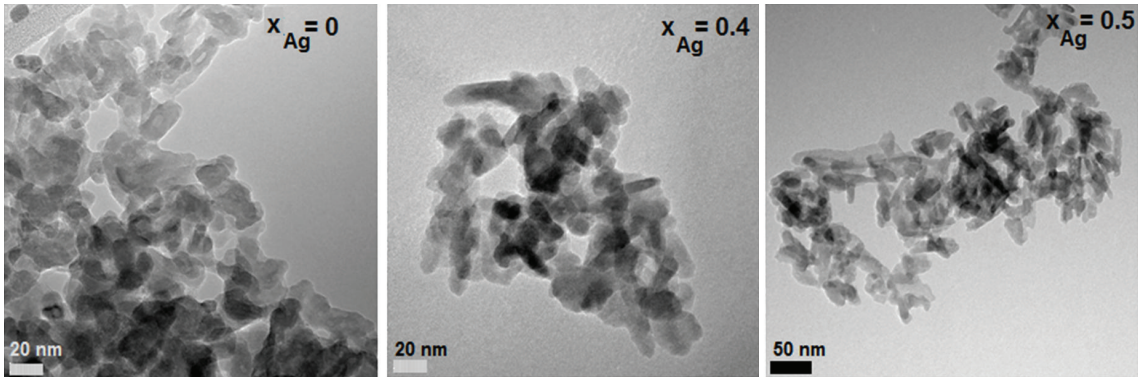

Figure 1: The TEM images of pure HAp ($x_{Ag} = 0$) and Ag:HAp ($x_{Ag} = 0.4$ and $x_{Ag} = 0.5$) with low resolution.

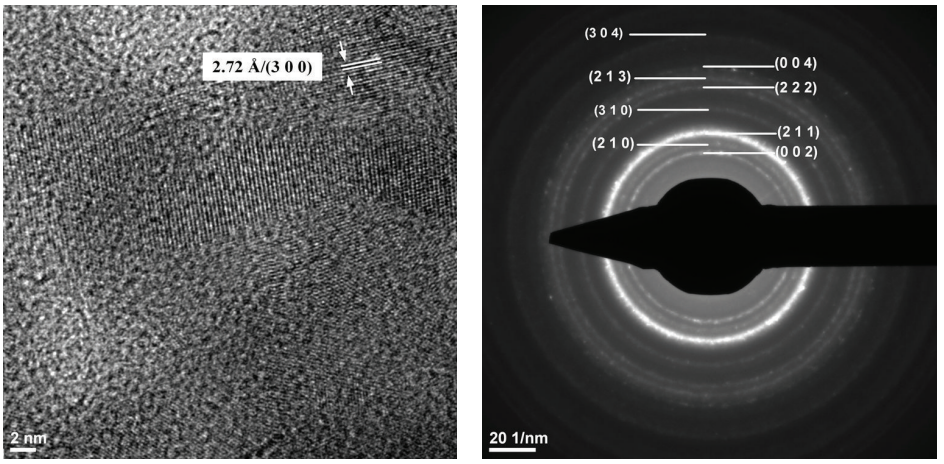

(a) (b)

Figure 2: HRTEM image and SAED analysis of Ag:HAp with $x_{Ag} = 0.5$.

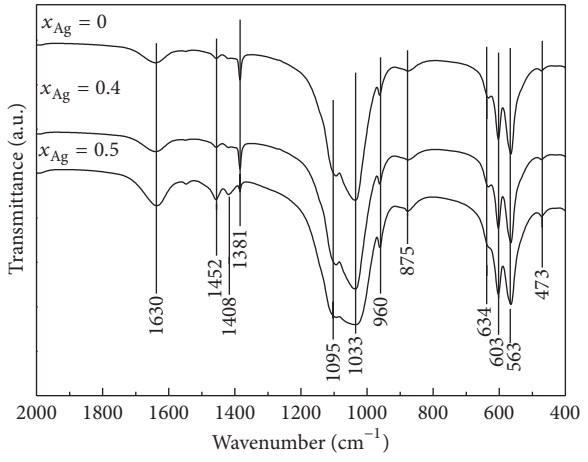

Figure 3: Transmittance infrared spectra of the Ag:HAp samples synthesized with $x_{Ag} = 0$, 0.4, and 0.5.

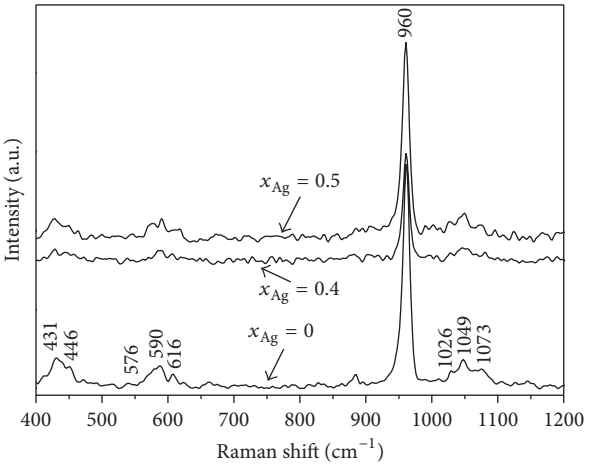

Figure 4: Raman spectra of the Ag:HAp samples synthesized with $x_{Ag} = 0$, 0.4, and 0.5.

band at 1073 cm^{-1}. The other CO_3 modes ν_3, ν_4, and ν_2 have band positions not obscured by the PO_4 bands, but they have weak intensities and were not detected [32]. Water vibrational modes give rise to weak intensity stretching and bending

Table 1: The results of the qualitative screening of the antimicrobial activity of Ag:HAp compounds against different *gram-positive* and *gram-negative* bacteria, as well as fungal strains.

Microbial strains			$x_{Ag} = 0$	$x_{Ag} = 0.4$	$x_{Ag} = 0.5$
Gram-negative strains	*Enterobacteriaceae* family	*E. coli* ATCC 25922	−	+	±
		E. coli 714	−	−	±
		K. pneumoniae 2968	−	+	+
		E. cloacae 61R	−	+	+
	Pseudomonadaceae family	*P. aeruginosa* 1397	±	+	±
Gram-positive strains	*Bacillaceae* family	*B. subtilis*	−	±	±
	Streptococcaceae family	*E. faecalis* ATCC 29212	−	−	−
	Micrococcaceae family	*S. aureus* 0364	−	+	+
Fungal strain		*C. krusei* 963	+	+	+

bands in Raman spectra. These water bands, expected at about the same wave number in FTIR spectra, were not observed in Raman spectra.

The qualitative antimicrobial activity of the tested compounds performed using stock solutions of 5 mg/mL obtained in dimethylsulfoxide (DMSO) allowed the selection of the active compounds, by the occurrence of high inhibition zones around the spotted compound. The results of the qualitative screening of the antimicrobial activity of Ag:HAp compounds against different *gram-positive* and *gram-negative* bacteria, as well as fungal strains are presented in Table 1. The tested compounds proved to be very active on *C. krusei* strain, irrespective of the Ag concentration. On the other hand, our tests proved them to be also active on *P. aeruginosa* 1397, *S. aureus* 0364, *K. pneumoniae* 2968, and *E. cloacae* 61R. The tested compounds, at certain concentrations, were also active against *E. coli 714*, *E. coli ATCC 25922,* and *B. subtilis*.

For the samples with $x_{Ag} = 0$ the antibacterial activity was not present in the case of *E. faecalis ATCC 29212, B. subtilis*, *E. coli ATCC 25922*, *K. Pneumoniae 2968*, *E. cloacae 61R,* and *S. aureus 0364 bacterial strains.* On the other hand it showed an inhibitory effect on the fungal strain *C. krusei 963* and the *gram-negative strain P. aeruginosa 1397*.

For $x_{Ag} = 0.4$, the tested samples presented a good antibacterial activity both on *gram-positive, gram-negative,* and fungal strains, excepting *E. coli 714 and E. faecalis ATCC 29212*.

The samples with $x_{Ag} = 0.5$ had a good antibacterial effect for all the tested microbial strains, except for E. faecalis ATCC29212.

4. Conclusions

Ag:HAp nanoparticles with $x_{Ag} = 0$, 0.4, and 0.5 were prepared by coprecipitation method at low temperature and characterized by TEM, FT-IR, and FT-Raman. TEM investigations confirmed the nanocrystalline nature of the synthesized powder and the ellipsometric morphology of the Ag:HAp particles. All 3 samples exhibit a uniform ellipsoidal morphology with particles from 5 nm to 15 nm. Bands characteristics of PO_4^{3-} tetrahedral apatite's structure are clearly observed by infrared and Raman analysis. The results of the qualitative screening of the antimicrobial activity of Ag:HAp compounds against different *gram-positive* and *gram-negative* bacterial strains proved to be very good irrespective of the Ag concentration. The specific antimicrobial activity revealed by the qualitative assay demonstrates that our compounds interacted differently with the microbial targets.

Acknowledgments

The authors would like to thank Professor Mariana Carmen Chifiriuc of Microbiology Immunology Department, Faculty of Biology, and University of Bucharest for assistance with antimicrobial tests and for the constructive discussions. This work was supported by the Ministry of Educations of the Romania, Project no. C2-06 under program CEA-IFA and Programul Nucleu PN 45.

References

[1] X. Renlong, L. Yang, C. Jiyong, and Z. Qiyi, "A comparative study of calcium phosphate formation on bioceramics in vitro and in vivo," *Biomaterials*, vol. 26, no. 33, pp. 6477–6486, 2005.

[2] W. J. E. M. Habraken, J. G. C. Wolke, and J. A. Jansen, "Ceramic composites as matrices and scaffolds for drug delivery in tissue engineering," *Advanced Drug Delivery Reviews*, vol. 59, no. 4-5, pp. 234–248, 2007.

[3] M. Vallet-Regí, F. Balas, M. Colilla, and M. Manzano, "Bioceramics and pharmaceuticals: a remarkable synergy," *Solid State Sciences*, vol. 9, no. 9, pp. 768–776, 2007.

[4] G. Binyamin, B. M. Shafi, and C. M. Mery, "Biomaterials: a primer for surgeons," *Seminars in Pediatric Surgery*, vol. 15, no. 4, pp. 276–283, 2006.

[5] M. W. Barsoum, *Fundamentals of Ceramics*, McGraw-Hill Series in Materials Science and Engineering, McGraw-Hill, edited by R. Gibala, M. Tirrell and C. A. West, 1997.

[6] J. E. Block and M. R. Thorn, "Clinical indications of calcium-phosphate biomaterials and related composites for orthopedic procedures," *Calcified Tissue International*, vol. 66, no. 3, pp. 234–238, 2000.

[7] K. S. Katti, "Biomaterials in total joint replacement," *Colloids and Surfaces B*, vol. 39, no. 3, pp. 133–142, 2004.

[8] Y. Huang, X. Jin, X. Zhang et al., "In vitro and in vivo evaluation of akermanite bioceramics for bone regeneration," *Biomaterials*, vol. 30, no. 28, pp. 5041–5048, 2009.

[9] A. R. Shahverdi, A. Fakhimi, H. R. Shahverdi, and S. Minaian, "Synthesis and effect of silver nanoparticles on the antibacterial activity of different antibiotics against *Staphylococcus aureus* and *Escherichia coli*," *Nanomedicine: Nanotechnology, Biology, and Medicine*, vol. 3, no. 2, pp. 168–171, 2007.

[10] N. J. Coleman, A. H. Bishop, S. E. Booth, and J. W. Nicholson, "Ag^{+}- and Zn^{2+}-exchange kinetics and antimicrobial properties of 11 Å tobermorites," *Journal of the European Ceramic Society*, vol. 29, no. 6, pp. 1109–1117, 2009.

[11] M. Guzman, J. Dille, and S. Godet, "Synthesis and antibacterial activity of silver nanoparticles against gram-positive and gram-negative bacteria," *Nanomedicine: Nanotechnology, Biology, and Medicine*, vol. 8, no. 1, pp. 37–45, 2011.

[12] A. W. Smith, "Biofilms and antibiotic therapy: is there a role for combating bacterial resistance by the use of novel drug delivery systems?" *Advanced Drug Delivery Reviews*, vol. 57, no. 10, pp. 1539–1550, 2005.

[13] C. S. Ciobanu, F. Massuyeau, L. V. Constantin, and D. Predoi, "Structural and physical properties of antibacterial Ag-doped nano-hydroxyapatite synthesized at 100∘C," *Nanoscale Research Letters*, vol. 6, Article ID 613, pp. 1–8, 2011.

[14] C. . Limban and M. C. Chifiriuc, "Antibacterial activity of new dibenzoxepinone oximes with fluorine and trifluoromethyl group substituents," *International Journal of Molecular Sciences*, vol. 12, no. 10, pp. 6432–6444, 2011.

[15] C. . Limban, L. Marutescu, M. C. Chifiriuc, and Synthesis, "Spectroscopic properties and antipathogenic activity of new thiourea derivatives," *Molecules*, vol. 16, no. 9, pp. 7593–7607, 2011.

[16] C. . Saviuc, A. M. Grumezescu, A. Holban et al., "Phenotypical studies of raw and nanosystem embedded *Eugenia carryophyllata* buds essential oil antibacterial activity on *Pseudomonas aeruginosa* and *Staphylococcus aureus* strains," *Biointerface Research in Applied Chemistry*, vol. 1, no. 3, pp. 111–118, 2011.

[17] M. C. . Chifiriuc, R. Palade, and A. M. Israil, "Comparative analysis of disk diffusion and liquid medium microdillution methods fortesting the antibiotic susceptibility patterns of anaerobic bacterial strains isolated from intrabdominal infections," *Biointerface Research in Applied Chemistry*, vol. 1, no. 6, pp. 209–220, 2011.

[18] L. . Marutescu, C. Limban, M. C. Chifiriuc, A. V. Missir, I. C. Chirita, and M. T. Caproiu, "Studies on the antimicrobial activity of new compounds containing thiourea function," *Biointerface Research in Applied Chemistry*, vol. 1, no. 6, pp. 236–241, 2011.

[19] D. Predoi, R. V. Ghita, F. Ungureanu, C. C. Negrila, R. A. Vatasescu-Balcan, and M. Costache, "Characteristics of hydroxyapatite thin films," *Journal of Optoelectronics and Advanced Materials*, vol. 9, no. 12, pp. 3827–3831, 2007.

[20] D. Predoi, M. Barsan, E. Andronescu, R. A. Vatasescu-Balcan, and M. Costache, "Hydroxyapatite-iron oxide bioceramic prepared using nano-size powders," *Journal of Optoelectronics and Advanced Materials*, vol. 9, no. 11, pp. 3609–3613, 2007.

[21] A. Costescu, I. Pasuk, F. Ungureanu et al., "Physico-chemical properties of nano-sized hexagonal hydroxyapatite powder synthesized by sol-gel," *Digest Journal of Nanomaterials and Biostructures*, vol. 5, no. 4, pp. 989–1000, 2010.

[22] S. M. Barinov, J. V. Rau, S. N. Cesaro et al., "Carbonate release from carbonated hydroxyapatite in the wide temperature rage," *Journal of Materials Science: Materials in Medicine*, vol. 17, no. 7, pp. 597–604, 2006.

[23] J. Qian, Y. Kang, W. Zhang, and Z. Li, "Fabrication, chemical composition change and phase evolution of biomorphic hydroxyapatite," *Journal of Materials Science: Materials in Medicine*, vol. 19, no. 11, pp. 3373–3383, 2008.

[24] C. S. Ciobanu, E. Andronescu, B. S. Vasile, C. M. Valsangiacom, R. V. Ghita, and D. Predoi, "Looking for new synthesis of hydroxyapatite doped with europium," *Optoelectronics and Advanced Materials, Rapid Communications*, vol. 4, no. 10, pp. 1515–1519, 2010.

[25] X. Bai, K. More, C. M. Rouleau, and A. Rabiei, "Functionally graded hydroxyapatite coatings doped with antibacterial components," *Acta Biomaterialia*, vol. 6, no. 6, pp. 2264–2273, 2010.

[26] A. Doat, F. Pellé, N. Gardant, and A. Lebugle, "Synthesis of luminescent bioapatite nanoparticles for utilization as a biological probe," *Journal of Solid State Chemistry*, vol. 177, no. 4-5, pp. 1179–1187, 2004.

[27] S. Koutsopoulos, "Synthesis and characterization of hydroxyapatite crystals. a review study on the analytical methods," *Journal of Biomedical Materials Research*, vol. 62, no. 4, pp. 600–612, 2002.

[28] J. Elliot, *Structural and chemistry of apatites and other calcium ortophosphates*, Elsevier, Amsterdam, The Netherlands, 1994.

[29] A. Mortier, J. Lemaitre, L. Rodrique, and P. G. Rouxhet, "Synthesis and thermal behavior of well-crystallized calcium-deficient phosphate apatite," *Journal of Solid State Chemistry*, vol. 78, no. 2, pp. 215–219, 1989.

[30] A. Mortier, J. Lemaitre, and P. G. Rouxhet, "Temperature-programmed characterization of synthetic calcium-deficient phosphate apatites," *Thermochimica Acta*, vol. 143, pp. 265–282, 1989.

[31] B. O. Fowler, "Infrared studies of apatites. I. Vibrational assignments for calcium, strontium, and barium hydroxyapatites utilizing isotopic substitution," *Inorganic Chemistry*, vol. 13, no. 1, pp. 194–207, 1974.

[32] M. Markovic, B. O. Fowler, and M. S. Tung, "Preparation and comprehensive characterization of a calcium hydroxyapatite reference material," *Journal of Research of the National Institute of Standards and Technology*, vol. 109, no. 6, pp. 553–568, 2004.